Next Energy 13 (2026) 100982

Contents lists available at ScienceDirect

Next Energy

journal homepage: www.sciencedirect.com/journal/next-energy

Research article

Impacts of stratospheric aerosol injection on renewable energy systems

Sebastian Kebrich[a,*,1], Luisa Kamp[a,*,1], Jochen Linßen[a], Heidi Heinrichs[a,b]

[a] Institute of Climate and Energy Research - Jülich Systems Analysis (ICE–2), Forschungszentrum Jülich GmbH, Wilhelm-Johnen Straße, Jülich, Nordrhein-Westfalen 52425, Germany
[b] Chair for Energy Systems Analysis, Department of Mechanical Engineering, University of Siegen, Paul-Bonatz Straße 9-11, Siegen, Nordrhein-Westfalen 57076, Germany

ARTICLE INFO

Keywords:
Solar geoengineering
Solar radiation management
Energy system optimization
Atmospheric aerosols
Energy transition

ABSTRACT

Climate change is one of the 21st century's major challenges. However, the progress in reducing greenhouse gas emissions is perceived as being too slow. Hence, more radical technologies such as stratospheric aerosol injection are entering discussions to limit climate change. This study presents a methodology for evaluating the effects of injecting 20Mt of SO_2 into the atmosphere annually on the global radiative balance, photovoltaic potentials, and renewable energy systems under a targeted temperature reduction of 2°C. Results show that the average annual reduction of photovoltaic (PV) potentials ranges from 0.25% to 4% up to 12% in Northern Europe during summer. The modeled renewable energy systems largely absorb these reductions resulting in minor capacity shifts with larger changes confined to a few systems. The results show that the inherent flexibility of large–scale renewable energy systems helps mitigating changes in cost, but understanding this flexibility is crucial to avoid errors in design.

1. Introduction

Global warming, driven by rising concentrations of greenhouse gases in the Earth's atmosphere, is one of the most critical challenges of this century [1]. According to the latest Copernicus Climate Report, the international goal of limiting global warming to between 1.5 and 2°C above pre-industrial levels was exceeded for the first time in 2024 [2]. Despite the steady increase in renewable energy technology capacity, with 447 GW of photovoltaic (PV) deployed in 2024 alone [3,4], the main source of energy remains conventional energy carriers like oil and gas. This has led to a steady increase in greenhouse gases since most countries plan to be greenhouse gas neutral by mid–century. This development underscores the intensified discourse on alternative approaches to mitigating the effects of global warming.

In this context, solar radiation management technologies are gaining increasing attention as potential tools to reduce the Earth's temperature by enhancing the reflectivity of incident solar radiation [5]. One such technology is Stratospheric Aerosol Injection (SAI), which is expected to reduce global temperatures by several degree and substantially offset the effects of climate change. It is also well understood due to its comparability to volcanic eruptions [6]. In this solar radiation management technology, sulfur dioxide (SO_2) is injected directly above the troposphere into the stratosphere to scatter incoming solar radiation. This alters the Earth's radiative balance, reducing direct irradiance while increasing diffuse irradiance and resulting in a net cooling effect on the atmosphere [7].

The cooling potential of SO_2 has recently been demonstrated by the impact of reduced emissions from ship tanks. Although these reductions were aimed at improving air quality, they contributed to a warming effect by reducing the reflection of solar radiation [8]. Despite the demonstrated cooling effects, however, the wider scientific and policy discourse on solar radiation management technologies remains divided. The 2024 expert report on solar radiation management outlines uncertainties and potential risks associated with these technologies, the lack of technology maturity needed, as well as not being suitable as a substitute for greenhouse gas reduction [2]. Nevertheless, the report emphasizes the need for increased research to fill significant gaps in knowledge, particularly on the direct and indirect effects of solar radiation management.

Previous research on SAI has focused on the atmospheric and climatic effects of induced SO_2, such as temperature patterns, atmospheric oscillations, and the carbon and hydrological cycle [6,9–11]. However, recent studies have also investigated secondary effects on social structures such as agriculture, water availability and geopolitical tensions [12]. Due to the direct relationship between solar irradiance and PV performance, a few studies have begun to examine the impact on PV

* Corresponding authors.
E-mail addresses: s.kebrich@fz-juelich.de (S. Kebrich), luisa.kamp@rwth-aachen.de (L. Kamp), j.linssen@fz-juelich.de (J. Linßen), h.heinrichs@fz-juelich.de (H. Heinrichs).

[1] These authors contributed equally to this work.

https://doi.org/10.1016/j.nxener.2026.100982
Received 28 January 2026; Received in revised form 28 August 2026; Accepted 1 September 2026

potentials [5,13,14]. These studies assume the injection of 5–15Mt SO_2 per year to offset 1–1. 5°C of global warming and use either the climate model Hadley Centre Global Environment Model [15] or the Coupled Model Intercomparison Project Phase 6 [16] for their calculations. These results show a reduction in PV potential between 1% and 7% globally [5,14], but the study on Nigeria reports increased radiation levels across the country except the coastal regions [13]. However, the possible reduction of PV performance due to SAI may therefore impact the needed renewable energy technology capacities [5].

SAI was selected based on a better understanding of its impact on different wavelengths, regional distribution, and seasonal dependency compared to other climate engineering technologies [11]. Additionally, its similarity to volcanic eruptions serves as a natural analogy, allowing for better estimation of the impact and support modeling of the technology [6]. Furthermore, although the aerosol injection process has to be repeated yearly due to sedimentation, the injection of 20Mt of sulfate precursors is estimated to be around $-2.5\frac{W}{m^2}$ corresponding to a temperature decrease of 2°C [10]. The injection process is simulated over a duration of ten years to establish an equilibrium state between injection, distribution and sedimentation. The injection location is along the equator, so that the aerosols can then be carried toward the North and South Poles by natural wind patterns, resulting in a rather uniform distribution worldwide. The remainder of the study, first examines the impact on the irradiance of SAI, then the impact on the resulting PV potentials, and finally the impact on energy systems worldwide, comparing systems that consider and do not consider the impact of SAI on PV potentials. The underlying methodology can be found in the appendix.

2. Results

The analysis covers three aspects. First, the global reduction in the radiative balance is presented. The average annual reduction ranges from $0.8\frac{W}{m^2}$ in (sub-)tropical regions and $3.1\frac{W}{m^2}$ beyond 50°N and 50°S, reaching up to $10\frac{W}{m^2}$ during the summer. Second, the impact on PV potentials is examined. The average yearly reduction lies between 2% and 4% for Northern America, Northern Europe and Northern Asia, but can be as high as 12% in Northern Europe during summer. Third, the impact on energy systems worldwide is evaluated by optimizing energy systems with and without the impact of SAI on PV potentials. The results show that large–scale energy systems absorb the impact largely, resulting in only minor capacity adjustment. Larger shifts are observed for a few, smaller energy systems.

2.1. Radiative balance changes are strongest during summer and beyond 50° North and South

Not only does the regional reduction of the radiative balance vary on average, it also varies greatly across seasons. Fig. 1 shows the mean annual reduction as well as the average seasonal reduction in direct irradiance ($\frac{W}{m^2}$) worldwide. The most affected areas include Northern Europe, Russia and parts of Canada, where annual average losses reach up to $3.1\frac{W}{m^2}$ compared to the case without SAI. This effect is similar to the global radiative forcing that the modeled SAI scenario aims to offset ($3.93\frac{W}{m^2}$). Similar intensities are observed in regions below 50°S, but, fewer countries are affected due to less land mass. The global spatial pattern is shaped by the dominant atmospheric circulations from the equator toward the poles. Although the aerosol injection point is near-equatorial to use the natural transport patterns from the equator the poles, a relatively weak exchange between tropical and extratropical regions leads to an accumulation in mid-latitudes. This results in characteristic belts of reduced irradiance around 20°N and 20°S, with typical average reductions of about $2\frac{W}{m^2}$ in direct irradiance, as shown in Fig. 1. SAI's effect on direct irradiance shows strong seasonal variations. Stronger reductions occur in regions below and above 50°S and 50°N during their respective spring and summer seasons as shown in Fig. 1, b-e. Tropical regions experience only minor reductions throughout the year, except near 20°N/S, where localized peaks occur in spring (March-May) due to aerosol transport patterns where the average irradiance reduction reaches up to $-6\frac{W}{m^2}$. Nonetheless, besides the accumulation between the tropics and the extratropics, the impact on the radiation in the tropics is around $-0.8\frac{W}{m^2}$.

2.2. Reduction of PV Potentials strongest during summer in the North

SAI-induced changes in the radiative balance result in a consistent global decrease in PV capacity factors that closely mirror the spatial patterns of direct irradiance losses. The strongest negative effects are observed in Norther America, Northern Europe, and Northern Asia, where aerosol transport toward the poles and increasing atmospheric variability lead to significant decreases. During summer, Northern Europe experiences a reduction of up to 12%, while reductions are between 2% and 4% during the remaining seasons. In Canada and Russia, reductions reach up to 6% during the summer and range from 2% to 4% throughout the rest of the year. The rest of the world experiences an average PV potential reduction of less than 1% on average, reaching around 2% in the area between the tropics and extratropics near 20°N/S during spring due to the accumulation of aerosols caused by the weak exchange between the two regions.

2.3. Flexibility in design of large–scale renewable energy system mostly compensate impacts of SAI

The total annual cost of energy systems worldwide remains effectively unchanged (-0.25%– $+0.5\%$), but shifts in capacity per technology can be identified. In most regions, the relative differences in capacity are below 10%, and especially large energy systems in terms of area and demand both — such as those covering North America, Europe, Northern Asia, China, and India — show only marginal adjustments. Larger shifts (10–20%) occur in four out of the 28 unions, while for one of the modeled unions, the overall design of its energy system changes more significantly.

2.3.1. Baseline renewable energy system configuration

Changes in PV potentials resulting from SAI were assessed for fully renewable energy systems worldwide in 2050. Energy systems were optimized for 28 unions allowing us to, on one hand, analyze the impact of SAI on 28 distinct and well defined scenarios, while, on the other hand, allowing the optimization to substitute technologies freely without the restrictions of existing capacities. For SAI itself we investigated two scenarios: one with standard PV potentials worldwide and one with PV potentials that include SAI–induced changes. All other parameters were held constant to isolate the impact of modified PV potentials on the overall system design. A brief model description can be found in the appendix, and a full description, including all union definitions, techno-economic parameters, and potentials, has been published by Franzmann et al. [17].

Fig. 3 shows these changes in capacity. Overall, several shifts are recognizable worldwide, with a few exceptions. As expected, there is a shift away from PV and toward wind, especially in North America, Europe, and Northern Asia, where the PV potential is reduced the most. Short-term storage increases, either via hydrogen gas vessels or lithium-ion batteries, while long-term storage relying on hydrogen decreases. Furthermore, the transmission of electricity is increasing worldwide in order to allow for greater flexibility when transferring large amounts of electricity over short timescales, in a manner similar to the growing deployment of short-term energy storage.

Similar to the changes in PV potential shown in Fig. 2, where North America, Northern Europe and Northern Asia have the highest changes of up to 4%, the reduction in PV capacity is up to 2%. Countries in

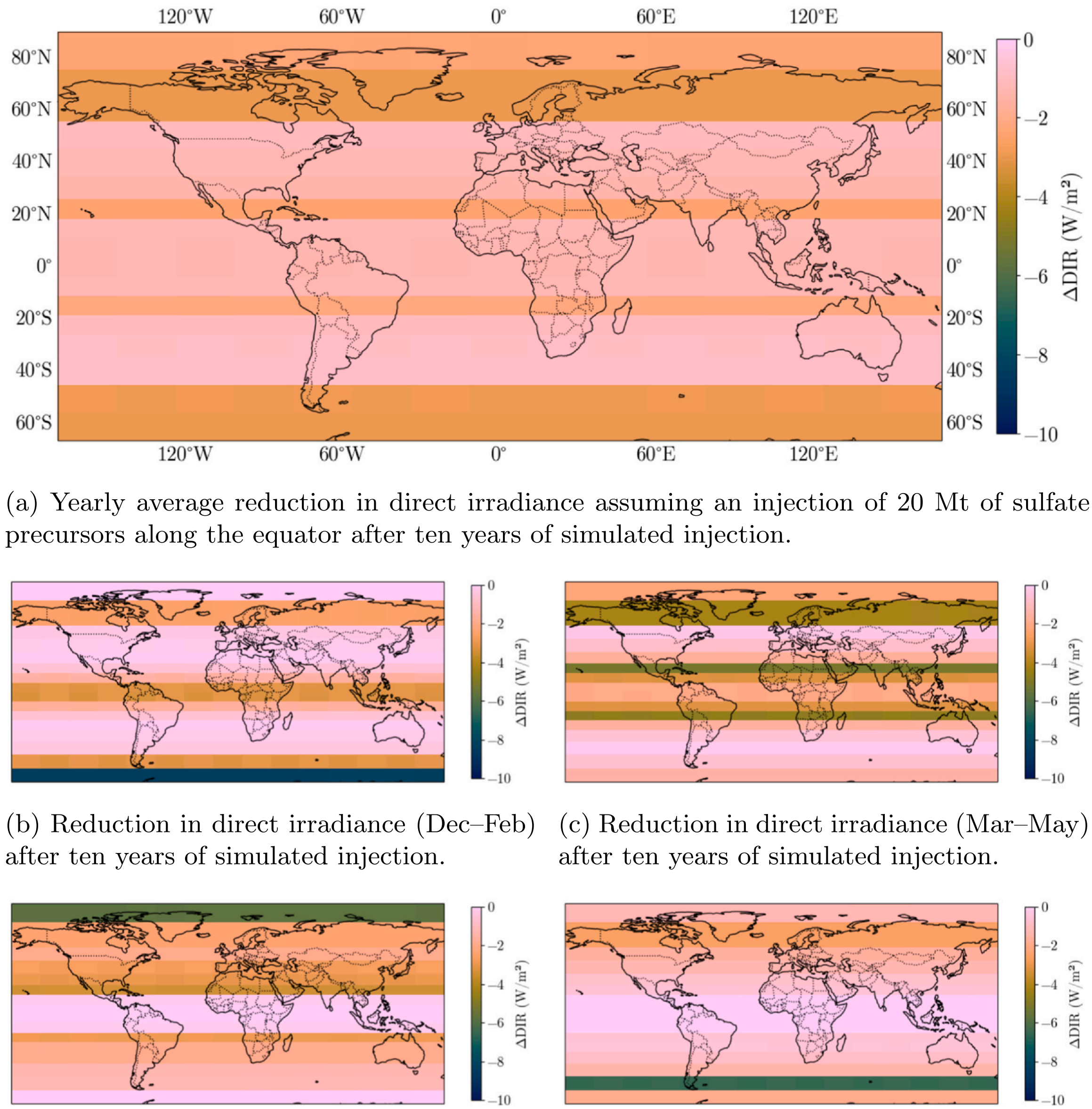

(a) Yearly average reduction in direct irradiance assuming an injection of 20 Mt of sulfate precursors along the equator after ten years of simulated injection.

(b) Reduction in direct irradiance (Dec–Feb) after ten years of simulated injection.

(c) Reduction in direct irradiance (Mar–May) after ten years of simulated injection.

(d) Reduction in direct irradiance (Jun–Aug) after ten years of simulated injection.

(e) Reduction in direct irradiance (Sep–Nov) after ten years of simulated injection.

Fig. 1. The reduction in direct irradiance is shown annually as well as seasonally after simulated injection of 20Mt of SO_2 in December annually for ten consecutive years to reach an equilibrium state between injection, distribution and sedimentation. Panel (a) shows the annual average reduction in direct irradiance (ΔDIR), ranging from $0.8\frac{W}{m^2}$ in the tropics to $3.1\frac{W}{m^2}$ starting around 50°S and 50°N. Around 20°S and 20°N an increased reduction of $2\frac{W}{m^2}$ arises from a weak tropical to subtropical exchange. Panels (b-e) show the seasonal mean changes in the same scenario. Reduction is high in the northern and southern hemisphere during the respective summer reaching up to $10\frac{W}{m^2}$. In the tropics the reduction is strongest directly in the month after injection in December with around $4\frac{W}{m^2}$ as shown in Panel (b). In the month from March to May shown in Panel (c) the reduction weakens and the belts around 20°S and 20°N form. In the remaining month from June to November the reduction in the tropics is negligible. The reduction starting around 20°S and 20°N is between $0.3\frac{W}{m^2}$ and $7.8\frac{W}{m^2}$ strongest during the summer in the month from June to November.

northern Europe, for example, rely more on energy from wind and geothermal, as well as on energy imports from PV in southern Europe, and are therefore less impacted. Greenland and Iceland, both island systems, demonstrate contrasting trends, with Greenland increasing its capacities for both PV and wind, while Iceland is reducing both. Iceland can rely on its vast geothermal potential; the country already relies on this resource, which provides about 95% of its energy, even without SAI. Greenland's energy system does not have this option and must therefore increase PV and wind capacities to compensate for reduced PV yield.

Two more modeled unions that show shifts larger than 10% are the union comprising Afghanistan and Pakistan and the union comprising Turkmenistan, Iran and Armenia. Both show similar shifts away from PV and towards wind energy. However, the former one increases its reliance on hydrogen gas turbines and vessel, while the latter one increased its reliance on Li–ion batteries.

An exceptionally large change occurs in the design of the Mexican energy system. Although the average capacity factor decreases by only 0.5% similar to the increase in total annual cost by 0.5%; the significant change in design indicates a high sensitivity to

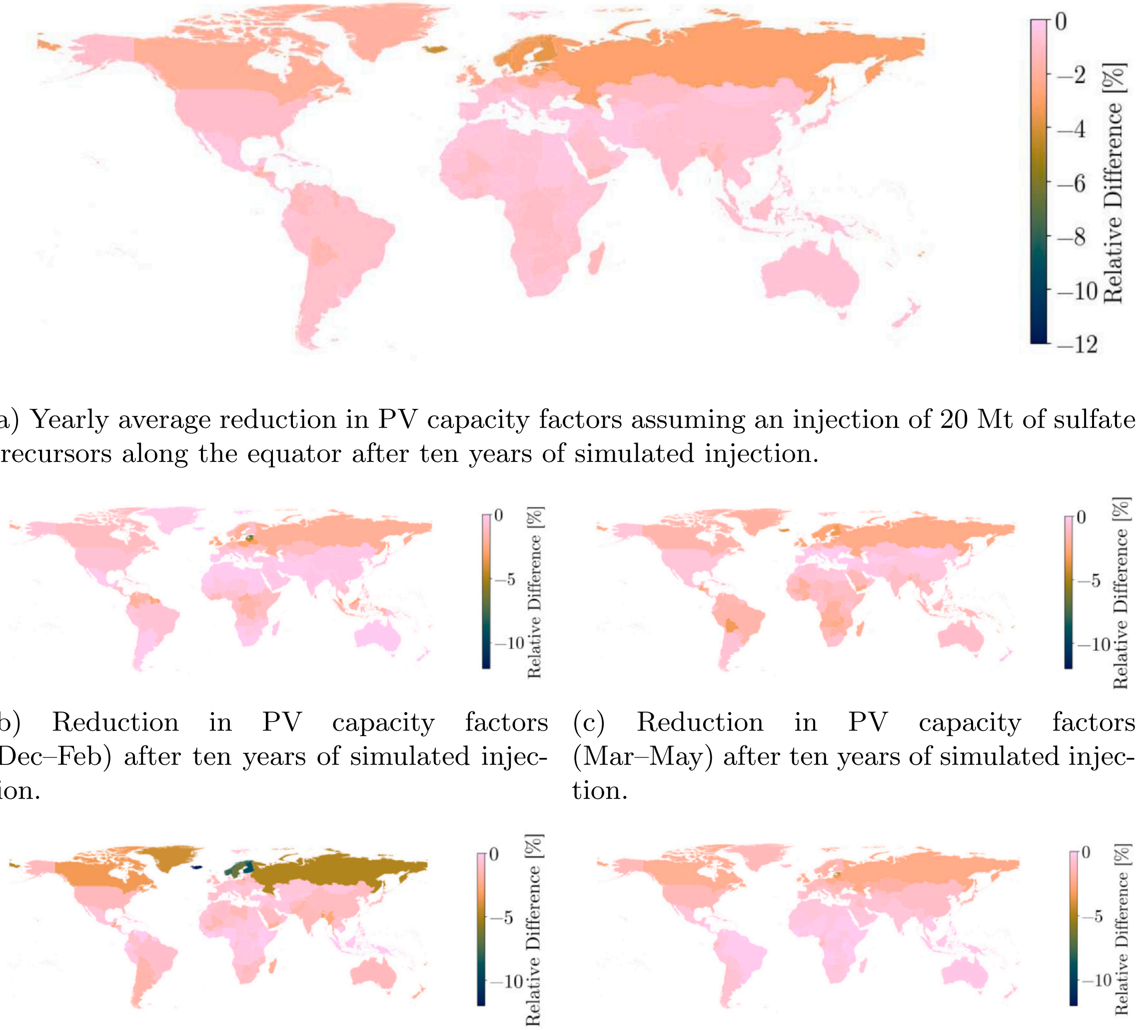

(a) Yearly average reduction in PV capacity factors assuming an injection of 20 Mt of sulfate precursors along the equator after ten years of simulated injection.

(b) Reduction in PV capacity factors (Dec–Feb) after ten years of simulated injection.

(c) Reduction in PV capacity factors (Mar–May) after ten years of simulated injection.

(d) Reduction in PV capacity factors (Jun–Aug) after ten years of simulated injection.

(e) Reduction in PV capacity factors (Sep–Nov) after ten years of simulated injection.

Fig. 2. The relative difference in PV capacity factors is shown annually as well as seasonally equivalently to the reduction in direct irradiance in Fig. 1. Panel (a) shows the relative annual average relative difference in PV capacity factors, ranging from 0.25% in the tropics to 4% Northern Europe. Panels (b-e) show the seasonal relative difference in the same scenario. Reduction is high in the northern hemisphere during the summer reaching up to 12% in Northern Europe. In the tropics the relative difference reaches up to 2% in the month after injection shown in Panel (b). In the month from March to May shown in Panel (c) the relative difference in the tropics weakens and instead spreads out to the subtropics. In the month from June to November the relative difference in the tropics reduces further and is negligible in the month from September to November. The relative difference in Northern America, Northern Europe and Northern Asia is similar throughout the year besides the summer, where it reaches up to 12%.

a reduction in its PV potential. Open field PV and geothermal capacities increase by 9% and 12%, respectively, while wind decreases by 12%. The change in capacities is even more pronounced for storage, the hydrogen sector, and transmission. Short–term storage increases for hydrogen vessels (+36%) and Li–ion batteries (+165%) while long–term storage in the form of hydrogen gas turbines (−15%) and hydrogen salt caverns (−15%) decreases, and electrolyzers (+6%) which for all other unions only shows minor changes.

In summary, the flexibility of energy systems, based on their combination of different technologies and large interconnected regions, mostly prevents cost changes. Some trends can be identified, such as the tendency to reduce PV, which aligns with the reduction of PV potentials. Only the Mexican energy system reacts with large-scale design changes, even though its PV potential reduction is minor.

3. Discussion

Although it has been demonstrated that SAI reduces surface solar irradiance and PV, as well as concentrated solar power potentials, its implications for energy systems have been largely unexplored. This study investigates the impact of SAI on PV potentials and on fully renewable energy systems worldwide. To the best of our knowledge, these investigations into energy systems are novel and extend existing literature by quantifying the necessary changes in their design.

The reduction in irradiation and corresponding PV potential is most notable in high-latitude regions. The most severe reductions in direct irradiation, up to $-10\frac{W}{m^2}$, occur during the summer in both the Northern and Southern Hemispheres, which reduces the impact on energy systems. The average reduction of the global PV potential ranges from 0.25% in tropical regions to 4% observed in areas such as North

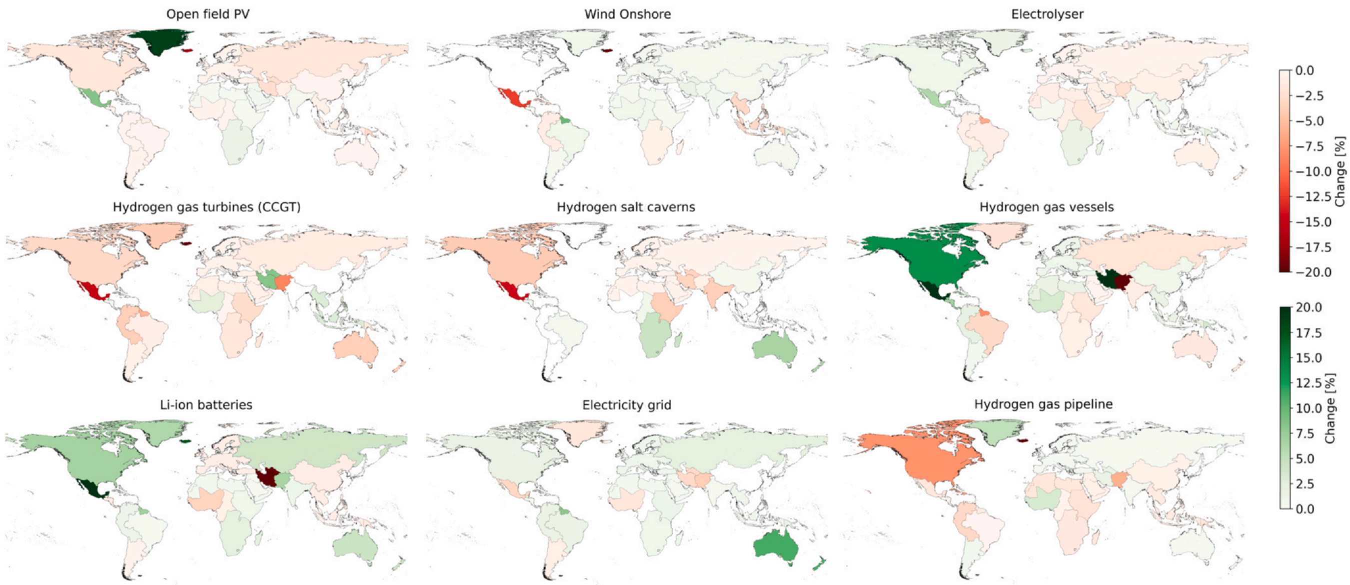

Fig. 3. The relative difference in the installed capacities of energy systems worldwide, split into 28 unions cut off at 20%, is shown. Geothermal energy is not depicted because the changes are negligible in all but one modeled union (Mexico). Changes are small for most unions (< 10%), especially for larger energy systems covering North America, Europe, and Northern Asia, as well as China and India. These systems show a slight shift from PV and long–term storage using hydrogen towards wind energy. There is an additional increase in transmission and short-term flexibility based on a slight increase in electricity transmission combined with an increase in either hydrogen vessels or Li–ion batteries. Larger shifts (10–20%) are observed in only five of the 28 unions, one of which (Mexico) shows significant changes in design. Greenland, Iceland, Afghanistan, and Pakistan, as well as Turkmenistan, Iran, and Armenia, show larger shifts (10–20%) in the relative shares of PV, wind, hydrogen gas turbines, hydrogen vessels, and Li-ion, respectively, but these technologies' overall share of operation is small, making up less than 10% of the energy system. Mexico's open field PV increases by 9%, similar to geothermal, which increases by 12%, while wind decreases by 12%. Furthermore, short–term storage flexibility increases for hydrogen vessels (+36%) and Li–ion batteries (+165%), while long–term storage in the form of hydrogen gas turbines (−15%) and hydrogen salt caverns (−15%) decreases.

America, northern Europe, and northern Asia. Similarly, the reduction in PV potential is strongest beyond 50°N and 50°S during the summer when the high availability can absorb the reductions well. The results of the two global studies in literature show a reduction in from 1% to 3% for the PV potential for an intended 1°C reduction [14] and from 1.4% to 6.9% for the PV potential for an intended 1.5–2°C reduction [5]. These results overlap in large parts with the results of 0.25–4% for this study with an intended temperature reduction of 2°C. The novel results on optimized energy systems based on renewable energy technologies worldwide demonstrate how flexibility in design, i.e. installed capacities, allows to absorb these impacts resulting in negligible changes in total annual cost (−0.25%– +0.5%).

Although the expected impact on PV's dominant role in energy systems is limited, consistent regional disparities drive subtle yet measurable shifts in the energy mix of these systems. The inherent flexibility of large-scale energy systems — capable of balancing generation from diverse sources — largely mitigates effects on total annual system costs. At the global scale, reduced irradiance and PV potentials slightly favor wind power expansion, indicating a marginal but systematic shift away from PV-dominated configurations toward more wind-based systems.

However, national systems with lower flexibility are more sensitive to these perturbations. Countries must therefore recognize the structural properties of their energy systems and their capacity to adapt to irradiance variability when designing long-term energy strategies. Mexico exemplifies this sensitivity: despite only minor reductions in PV potential, its optimal system configuration changes markedly, underscoring how small shifts in solar resources can propagate through system design choices. These changes in design stem from the vast renewable potentials available for PV, wind and geothermal energy due to the position close to the equator as well as being surrounded by oceans. This allows for larger trade offs among energy sources, here a shift towards PV and geothermal energy. The remaining changes are attributed to this shift; PV and geothermal energy are more reliant on short term storage since their (daily) patterns are more reliable than wind generation, which in turn relies more on longer term storage of energy using hydrogen gas turbines and salt caverns. The shift towards especially PV can therefore be explained by its predictable electricity generation rather than the minor reduction in potential. While in this study, the modeled unions are mostly large-scale energy systems, real-world transitions may lead to more distributed and regionally autonomous configurations, likely enhancing the observed shifts.

The scope of this work is limited to the effects of SAI on PV potentials and its impact on renewable energy systems. SAI likely impacts other energy sources, such as wind, biomass and hydro power, which in turn impacts energy systems based on these technologies. While the global impact on wind power might be negligible, regional changes are estimated to be as high as 16% [18]. Further, their models show more weeks of low production per year, likely increasing the difficulty to supply sufficient electricity during lull and dark lull periods. For bioenergy an overall improvement is expected. The combination of reduced heat, but increased CO_2 levels are likely to increase production of biomass [19], further supported by the increase in diffuse irradiation [20]. For hydro power it is expected that the impact of climate change is reduced. The melting of glaciers would be slowed, aridity reduced and precipitation stabilized [21,22], likely increasing the reliability of hydro power. Another aspect, and a major source of uncertainty of SAI, which is not covered in this work, is the impact on cloud formation in the troposphere. According to literature the impact on cloud formation is expected to be the largest in the tropics [23–25] and the monsoon regions [26,27] with an overall reduction of cloud systems. This would counteract the already small changes in PV potentials in these regions and likely lead to an overall increase. The impact on other regions is heterogeneous and weaker than in the tropics. Beyond its impact on energy systems, the consequences of increasing CO_2 levels themselves in the atmosphere and the oceans are not offset, especially if SAI discourages decision-makers from reducing CO_2 output. The consequences of stopping SAI (termination shock), resulting in a short–term temperature increase similar to the reduction caused by SAI, are not part of this work, but need to be carefully considered to avoid unwanted and potentially severe consequences. Our analysis suggests that the impact on the energy systems following such a termination shock itself would be moderate at worst. While the system configurations would be non optimal, the reduction in PV potential generally caused an increase in cost, meaning additional capacities are built. Using these, and adjusting the operational schedule using the flexibility of renewable energy systems likely prevent any kind of larger supply gaps.

The resulting renewable energy systems are strongly dependent on the underlying cost assumptions used in the optimization. Different assumptions would lead to different energy system designs favoring relatively cheaper technologies. The effect of varying cost assumptions is instead reflected by the diversity of conditions represented across the 28 unions. While the cost assumptions are kept constant across the unions, they differ substantially in their respective renewable potentials, resulting in variations in capacity factors, full-load hours, and seasonal generation profiles. PV as well as wind potentials vary over several orders of magnitude from negligible in Micronesia to hundreds of PWh_{el} in North America. CSP changes similarly to the PV potentials and geothermal is not available for two unions, while reaching over $10PWh_{el}$ for Noth America, South-East Asia and Australia and New Zealand. Similarly, the demand changes from $10\,TWh_{el}$ for Micronesia to $10PWh_{el}$ for China and North America. Hydrogen storage is not available for 11 unions, while Australia and New Zealand as well as North America have the potential to store hundreds of PWh_{H_2}. This in turn leads to different technologies being advantageous for different unions, similar to different cost scenarios. The impact of changes in transmission cost is reflected in the different size of unions and the employment of storage capacities depend on the availability of salt caverns in combination with electricity generation. Energy systems with lots of electricity generation from wind depend more on hydrogen to cover lulls, while PV is usually associated with batteries. The overall consistent changes in cost and also design of energy systems with only a few notable exceptions such as the Mexican one discussed before approximate the sensitivity to changes in cost of technologies. This consistency suggests that the conclusions are robust to a large range of operational parameter.

A limitation of the present approach is that the adopted aerosol parameterization is based on observations from a volcanic eruption. While the adopted tropical injection as well as the distribution formulation and aerosol effective radius are idealizations sufficient for our study, which is mainly focused on the interaction of SAI with energy systems, recent studies have shown that the spatial distribution of sulfate aerosols produced by SAI depends strongly on injection latitude, season, and the representation of stratospheric transport and the aerosols themselves. Tropical and off-equatorial injections can produce different distributions of aerosols and would impact fully renewable energy systems differently [28,29]. Moreover, continuous sulfur injection generally promotes particle growth through condensation and coagulation, resulting in larger effective radii than those observed following individual volcanic eruptions, with potential implications for aerosol optical properties, sedimentation rates, and radiative forcing. The assumed aerosol effective radius and distribution width may therefore underestimate particle sizes expected under sustained SAI conditions. Finally, while tropical injection is frequently adopted in idealized SAI studies, recent work has shown that it is not necessarily the optimal deployment strategy. Multi-location injection schemes spanning tropical and subtropical latitudes can provide greater control over aerosol spatial distributions and radiative forcing patterns [30,31].

Future research on the impacts of SAI on energy systems should focus on energy systems that are either regionally constrained or have limited demand as both limit their inherent flexibility. Further, it is also needed to quantify how SAI affects other renewable energy potentials like wind and hydropower, and how these combined changes impact the energy system configuration.

Code availability

The python code is to calculate the changes in radiative balance and the PV potentials is available on github at Reskit - Stratospheric Aerosol Injection. A full description of the energy system model used can be found in Franzmann et al. [17].

CRediT authorship contribution statement

Heidi Heinrichs: Writing – review & editing, Supervision, Funding acquisition, Conceptualization. **Linßen Jochen:** Writing – review & editing, Resources. **Luisa Kamp:** Writing – original draft, Visualization, Validation, Software, Methodology, Investigation, Formal analysis, Data curation. **Sebastian Kebrich:** Writing – review & editing, Writing – original draft, Visualization, Validation, Methodology, Investigation, Formal analysis, Conceptualization.

Declaration of Competing Interest

The authors declare that they have no known competing financial interests or personal relationships that could have appeared to influence the work reported in this paper.

Declaration of generative AI and AI-assisted technologies in the writing process

During the preparation of this work the authors used Perplexity AI, ChatGPT (GPT-4) and DeepL Write in order to improve clarity and language. After using this tool/service, the authors reviewed and edited the content as needed and take full responsibility for the content of the published article.

Acknowledgements

This work was supported by the Helmholtz Association as part of the Platform for the Design of a Robust Energy System and Raw Material Supply (RESUR) and the program, “Energy System Design.”

This work was partly funded by the European Union (ERC, MATERIALIZE, 101076649). Views and opinions expressed are however those of the authors only and do not necessarily reflect those of European Union or the European Research Council Executive Agency. Neither the European Union nor the granting authority can be held responsible for them.

Appendix A. Supporting information

Supplementary data associated with this article can be found in the online version at doi:10.1016/j.nxener.2026.100982.

References

[1] IRENA, Global hydrogen trade to meet the 1.5°C climate goal: Part III - Green hydrogen cost and potential, tech. rep., International Renewable Energy Agency, Abu Dhabi, 2022.
[2] C. C. C. S. (C3S), Global Climate Highlights 2024, tech. rep., 2025.
[3] IRENA, World Energy Transitions Outlook 2023: 1.5°C Pathway, Tech. Rep. 1, Abu Dhabi.
[4] T. Dunster, Global Market Outlook for Solar Power.
[5] S. Baur, B.M. Sanderson, R. Séférian, L. Terray, Solar radiation modification challenges decarbonization with renewable solar energy, Earth Syst. Dyn. 15 (2024) 307–322.
[6] H.N. Huynh, V.F. McNeill, The potential environmental and climate impacts of stratospheric aerosol injection: a review, Environmental Science Atmospheres 4 (2) (2024) 114–143.
[7] O. Bochuer, 7: Clouds and Aerosols, Climate Change 2013: The Physical Science Basis, IPCC 2013, Cambridge University Press, Cambridge, United Kingdom and New York, NY, USA, 2013.
[8] Z. Hausfather and P.M. Forster, Analysis: How low-sulphur shipping rules are affecting global warming, 2023.
[9] P.J. Irvine, B. Kravitz, M.G. Lawrence, H. Muri, An overview of the Earth system science of solar geoengineering, WIREs Clim. Change 7 (2016) 815–833.

[10] H. Muri, J. Tjiputra, O.H. OtterÅ, M. Adakudlu, S.K. Lauvset, A. Grini, M. Schulz, U. Niemeier, J.E. Kristjánsson, Climate response to aerosol geoengineering: a multimethod comparison, J. Clim. 31 (2018) 6319–6340.
[11] J.M. Moch, L.J. Mickley, S.D. Eastham, E.W. Lundgren, V. Shah, J.J. Buonocore, J.Y.S. Pang, M. Sadiq, A.P.K. Tai, Overlooked long-term atmospheric chemical feedbacks alter the impact of solar geoengineering: implications for tropospheric oxidative capacity, AGU Adv. 4 (2023) e2023AV000911.
[12] A. Kumler, B. Kravitz, C. Draxl, L. Vimmerstedt, B. Benton, J.K. Lundquist, M. Martin, H.J. Buck, H. Wang, C. Lennard, L. Tao, Potential effects of climate change and solar radiation modification on renewable energy resources, Renew. Sustain. Energy Rev. 207 (2025) 114934.
[13] O. Ojo, I. Emmanuel, E. Ogolo, B. Adeyemi, Impact of stratospheric aerosol injection on photovoltaic energy potential over Nigeria, Asian, J. Atmos. Environ. 18 (2024) 5.
[14] C.J. Smith, J.A. Crook, R. Crook, L.S. Jackson, S.M. Osprey, P.M. Forster, Impacts of stratospheric sulfate geoengineering on global solar photovoltaic and concentrating solar power resource, J. Appl. Meteorol. Climatol. 56 (2017) 1483–1497.
[15] G.M. Martin, M.A. Ringer, V.D. Pope, A. Jones, C. Dearden, T.J. Hinton, The physical properties of the atmosphere in the new Hadley Centre Global Environmental Model (HadGEM1). Part I: model description and global climatology, J. Clim. 19 (7) (2006) 1274–1301.
[16] E.K. Makula, B. Zhou, Coupled model intercomparison project phase 6 evaluation and projection of East African precipitation, Int. J. Climatol. 42 (4) (2022) 2398–2412.
[17] D. Franzmann, C. Winkler, P. Dunkel, M. Stargardt, A. Burdack, S. Ishmam, J. Linßen, D. Stolten, and H. Heinrichs, Impact of spatial aggregation on global renewable energy system with ethos. modelbuilder, Available at SSRN 5252316, 2025.
[18] Susanne BAUR, et al., Change in wind renewable energy potential under stratospheric aerosol injections, Earth's Future 12 (10) (2024) e2024EF004575.
[19] K. Dagon, Schrag D.P, Quantifying the effects of solar geoengineering on vegetation, Clim. Change 153 (1) (2019) 235–251.
[20] L. Xia, A. Robock, D.K. Visioni, et al., Solar radiation management impacts on agriculture in China: a case study in the Geoengineering Model Intercomparison Project (GeoMIP), J. Geophys. Res. Atmospheres 119 (14) (2014) 8695–8711.
[21] O. Boucher, R.D. Jones, P.M. Forster, Climate engineering and the hydrological cycle, Nat. Clim. Change 3 (4) (2013) 363–365.
[22] S. Tilmes, J.H. Richter, M.J. Mills, et al., Effects of different stratospheric aerosol injection strategies on surface temperature and hydrological cycle changes, J. Geophys. Res. Atmospheres 123 (11) (2018) 6434–6458.
[23] Huynh, T., and McNeill, V.F. (2024). The potential environmental and climate impacts of stratospheric aerosol injection: a review.(Review article on SAI-climate interactions, including cloud and hydrological responses).
[24] McGraw, Z., and Polvani, L.M. (2025). Direct radiative impacts of stratospheric aerosols on the tropical troposphere: clouds, precipitation, and circulation in convection-resolving and global simulations.(Study of SAI-induced changes in tropical convection, cloud formation, and rainfall).
[25] A. Robock, Volcanic eruptions and climate, Rev. Geophys. 38 (2) (2000) 191–219, https://doi.org/10.1029/1998RG000054.
[26] E.M. Bednarz, et al., Climate response to off-equatorial stratospheric sulfur injections in three Earth system models - Part 2, Atmos. Chem. Phys. 23 (2023) 687–709, https://doi.org/10.5194/acp-23-687-2023.
[27] C. Sun, et al., Global monsoon response to tropical and Arctic stratospheric aerosol injection, Clim. Dyn. (2020), https://doi.org/10.1007/s00382-020-05371-7.
[28] D. Visioni, E.M. Bednarz, W.R. Lee, B. Kravitz, A. Jones, J.M. Haywood, D.G. MacMartin, Climate response to off-equatorial stratospheric sulfur injections in three Earth system models – Part 1: Experimental protocols and surface changes, Atmos. Chem. Phys. 23 (2023) 663–686, https://doi.org/10.5194/acp-23-663-2023.
[29] E.M. Bednarz, D. Visioni, B. Kravitz, A. Jones, J.M. Haywood, J. Richter, D.G. MacMartin, P. Braesicke, Climate response to off-equatorial stratospheric sulfur injections in three Earth system models – Part 2: Stratospheric and free-tropospheric response, Atmos. Chem. Phys. 23 (2023) 687–709, https://doi.org/10.5194/acp-23-687-2023.
[30] D.G. MacMartin, B. Kravitz, S. Tilmes, J.H. Richter, M.J. Mills, J.-F. Lamarque, J.J. Tribbia, F. Vitt, The climate response to stratospheric aerosol geoengineering can be tailored using multiple injection locations, J. Geophys. Res. Atmospheres 122 (2017) 12574–12590, https://doi.org/10.1002/2017JD026868.
[31] B. Kravitz, D.G. MacMartin, M.J. Mills, J.H. Richter, S. Tilmes, J.-F. Lamarque, J.J. Tribbia, F. Vitt, First simulations of designing stratospheric sulfate aerosol geoengineering to meet multiple simultaneous climate objectives, J. Geophys. Res. Atmospheres 122 (2017) 12616–12634, https://doi.org/10.1002/2017JD026874.